Acta Neuropathol (2006) 112:405–415
DOI 10.1007/s00401-006-0115-3

ORIGINAL PAPER

RAGE, LRP-1, and amyloid-beta protein in Alzheimer's disease

John E. Donahue · Stephanie L. Flaherty · Conrad E. Johanson · John A. Duncan III · Gerald D. Silverberg · Miles C. Miller · Rosemarie Tavares · Wentian Yang · Qian Wu · Edmond Sabo · Virginia Hovanesian · Edward G. Stopa

Received: 24 April 2006 / Revised: 30 June 2006 / Accepted: 1 July 2006 / Published online: 25 July 2006

Abstract The receptor for advanced glycation end products (RAGE) is thought to be a primary transporter of β-amyloid across the blood–brain barrier (BBB) into the brain from the systemic circulation, while the low-density lipoprotein receptor-related protein (LRP)-1 mediates transport of β-amyloid out of the brain. To determine whether there are Alzheimer's disease (AD)-related changes in these BBB-associated β-amyloid receptors, we studied RAGE, LRP-1, and β-amyloid in human elderly control and AD hippocampi. In control hippocampi, there was robust RAGE immunoreactivity in neurons, whereas microvascular staining was barely detectable. LRP-1 staining, in contrast, was clearly evident within microvessels but only weakly stained neurons. In AD cases, neuronal RAGE immunoreactivity was significantly decreased. An unexpected finding was the strongly positive microvascular RAGE immunoreactivity. No evidence for colocalization of RAGE and β-amyloid was seen within either microvessels or senile plaques. A reversed pattern was evident for LRP-1 in AD. There was very strong staining for LRP-1 in neurons, with minimal microvascular staining. Unlike RAGE, colocalization of LRP-1 and β-amyloid was clearly present within senile plaques but not microvessels. Western blot analysis revealed a much higher concentration of RAGE protein in AD hippocampi as compared with controls. Concentration of LRP-1 was increased in AD hippocampi, likely secondary to its colocalization with senile plaques. These data confirm that AD is associated with changes in the relative distribution of RAGE and LRP-1 receptors in human hippocampus. They also suggest that the proportion of amyloid within the brains of AD patients that is derived from the systemic circulation may be significant.

Keywords Alzheimer's disease · Blood–brain barrier · Amyloid-β-protein · Receptor for advanced glycation end products · Low-density lipoprotein receptor-related protein-1

J. E. Donahue · S. L. Flaherty · C. E. Johanson · J. A. Duncan III · M. C. Miller · R. Tavares · Q. Wu · E. G. Stopa
Department of Clinical Neurosciences, Rhode Island Hospital and Brown Medical School, Providence, RI, USA

G. D. Silverberg
Department of Neurosurgery, Stanford University Medical Center and School of Medicine, Stanford, CA, USA

W. Yang
Cancer Biology Program, Division of Hematology-Oncology, Department of Medicine, Beth Israel-Deaconess Medical Center and Harvard Medical School, Boston, MA, USA

E. Sabo
Molecular Pathology Core, COBRE CCRD, Rhode Island Hospital and Brown Medical School, Providence, RI, USA

V. Hovanesian
Core Image Analysis Laboratory, Rhode Island Hospital, Providence, RI, USA

J. E. Donahue (✉)
Division of Neuropathology, Department of Pathology, Rhode Island Hospital, 593 Eddy Street (APC 12115), Providence, RI, 02903, USA
e-mail: JDonahue3@Lifespan.org

Introduction

The source of the amyloid-β (Aβ) burden in the brains of patients with Alzheimer's disease (AD) is controversial. Many researchers favor a neuronal or neuritic origin [14], but there may actually be several different origins. The glia may make a contribution [23], though this is likely inconsequential compared to other possible sources such as the systemic circulation [12, 18]. Increased levels of Aβ on plasma lipoproteins and proteins in AD suggest that circulating Aβ could be a precursor of brain Aβ [32].

While some circulating Aβ may enter the brain via a "leaky" blood–brain barrier (BBB) [24], active transport of Aβ across the BBB does occur [11], where a number of Aβ receptors have been discovered [10, 13]. Two of the better characterized are the receptor for advanced glycation end products (RAGE) [6] and the low-density lipoprotein receptor-related protein (LRP)-1 [20]. RAGE is a multi-ligand receptor in the immunoglobulin superfamily of cell surface molecules. It binds a wide range of molecules, including the products of nonenzymatic glycoxidation (advanced glycation end products, or AGEs), Aβ, proinflammatory cytokine-like mediators in the S-100/calgranulin family, and a DNA-binding protein, amphoterin [29]. LRP-1 is a member of the LDL receptor family. It functions both as a multi-functional scavenger and signaling receptor and as a transporter and metabolizer of cholesterol and apolipoprotein E (apoE)-containing lipoproteins [9]. Like RAGE, LRP-1 binds a wide range of ligands, including apoE, α_2-macroglobulin, amyloid precursor protein, and Aβ [32]. Transport of Aβ from the bloodstream into the brain is mediated by RAGE [6], and Aβ transport from the brain into the bloodstream is mediated by LRP-1 [20]. The net flux of Aβ into or out of the brain is the algebraic sum of the inward flux and outward flux and presumably depends upon the density and activity of these two receptors.

Experiments defining the functions of RAGE and LRP-1 described above have been performed in mice [6, 20]. This study attempts to explore both RAGE and LRP-1 in human brain tissue and to determine whether there are AD-related changes in these BBB-associated Aβ receptors that might shed light on the mechanism(s) of Aβ accumulation.

Materials and methods

Human tissues

All brains (AD, $n = 6$, mean age = 79 ± 7 years, three male, three female; normal aged controls, $n = 6$, mean age = 70 ± 8 years, three male, three female) were obtained at autopsy (postmortem interval, 2–24 h). Tissue was obtained from both the Brown Brain Bank and the Harvard Brain Tissue Resource Center. The diagnosis of AD was made in accordance with widely accepted National Institute on Aging Criteria [1], as well as the Braak and Braak neuropathological staging of Alzheimer-related changes [2]. In this study, all AD brains were diagnosed as having Braak and Braak stage V–VI disease, the most severe form of AD. Control brains were obtained from aged hospital patients with no history of neurological disease and no pathologic evidence of AD or other degenerative brain diseases, even in the earliest stages.

Samples of hippocampus were fixed by immersion in 4% paraformaldehyde in 0.1 M phosphate buffer (pH 7.4) for 24 h and cryoprotected with 30% sucrose in 0.1 M phosphate buffer (pH 7.4). Samples then were snap-frozen in liquid nitrogen and stored at −70°C until they were used.

Immunofluorescence

Fixed-frozen tissue samples of human hippocampi were embedded in OCT compound, sectioned at 50 μm, and rinsed in Tris-buffered saline (TBS). Sections were then incubated for 1 h in 5% normal serum (Vector Laboratories), of either rabbit (RAGE) or goat (LRP-1). After incubation with primary antibody for 24 h (RAGE 1:400 dilution, Research Diagnostics Inc.; LRP-1 1:500 dilution, Orbigen Inc.; neurofilament 1:100 dilution, Novocastra; CD31 1:100 dilution, Research Diagnostics Inc.), tissue sections were washed and stained with an appropriate secondary antibody conjugated to either Cy2 or Cy3 (Jackson ImmunoResearch) and then rinsed in TBS. For Aβ colocalization experiments, sections were then rinsed in 70% ethanol and incubated for 30 min in 0.1% thioflavin S (Sigma), rinsed for 15 min in 70% ethanol, and incubated for 30 min in 0.7% Sudan Black B (Sigma) to eliminate autofluorescence from tissue lipofuscin. Sections were finally rinsed in distilled water, mounted onto glass slides with 0.1% gelatin, and cover-slipped with Vectashield mounting medium (Vector Laboratories).

Quantitative Immunohistochemistry

For quantitative RAGE immunohistochemical studies, 5 μm paraffin hippocampal sections were cut, mounted on Superfrost Plus glass slides, and placed in a 60°C degree oven for 1 h. Sections were then deparaffinized and quenched with peroxidase blocking reagent (Dako Cytomation) for 20 min at room temperature to

eliminate endogenous peroxidase activity. This was followed by blocking overnight with 10% normal rabbit serum in Tris buffer. Sections were then incubated with avidin (Vector Laboratories) for 15 min, briefly rinsed with Tris buffer, and then incubated with biotin (Vector Laboratories) for an additional 15 min. Sections were then rinsed three times in Tris buffer for 5 min for each wash and incubated with primary RAGE antibody (Research Diagnostics Inc.) at 1:75 dilution overnight in a humidity chamber placed in a refrigerator (at 4°C). After primary incubation, sections were rinsed in Tris buffer as above and inoculated with anti-goat IgG biotinylated secondary antibody (Vector Laboratories) for 30 min at room temperature. Sections were then rinsed in Tris buffer as above. For detection of primary antibody, slides were treated with avidin-biotin complex (ABC) (Vector Laboratories) for 30 min. Slides were then incubated with diaminobenzidine (DAB) as the chromagen for 5 min for visualization. No counterstain was used. Slides were coverslipped with Cytoseal (Stevens Scientific).

For quantitative LRP-1 immunohistochemical studies, 5 μm paraffin hippocampal sections were cut, mounted on Superfrost Plus glass slides, and placed in a 60°C degree oven for 1 h. Sections were then deparaffinized and incubated with target retrieval solution (Dako Cytomation) diluted 1:10 with distilled water in a pressure cooker in the microwave on high for 11 min. Sections were allowed to come to room temperature over 30 min and then washed with distilled water three times for 3 min each. This was followed by quenching with peroxidase blocking reagent (Dako Cytomation) for 20 min at room temperature to eliminate endogenous peroxidase activity. Sections were then washed three times with Tris buffer (3 min each) and incubated with normal goat serum (diluted 1:10 with Tris buffer) overnight in a 4°C refrigerator. Then sections were incubated overnight with primary LRP-1 antibody (Orbigen Inc.) at 1:75 dilution in a 4°C refrigerator. Sections were then rinsed three times with Tris buffer as above and incubated with labeled polymer-HRP (anti-rabbit HRP—horseradish peroxidase; Dako Cytomation) for 30 min at room temperature. This was followed by three rinses with Tris buffer as above and incubation with substrate-chromagen (DAB) for 5 min. No counterstain was used. Sections were then washed with tap water, rinsed three times with distilled water, and coverslipped with Cytoseal (Stevens Scientific).

Quantitative image analysis

Immunohistochemically-stained slides were scanned using a light microscope (Olympus BX41, Olympus Optical Co. Ltd., Tokyo, Japan) at a 400× magnification. The microscopic images were captured with a digital camera (MicroPublisher 3.3 RTV, QIMAGING, Burnaby, BC, Canada). In each case, between five and ten mostly intense microscopic fields were submitted for the quantitative analysis. Image ProPlus 6.0 (MediaCybernetics, Silver Spring, MA, USA) software was used to segment and measure the intensity of pixels in the green channel, representing the cytoplasm of the neurons and vascular endothelial cells. Pixel intensities (OD: optical density) ranged from 0 (most densely-stained pattern; i.e., black) to 255 (most lightly-stained pattern; i.e., white). Comparison of the gray levels between each two parametric groups was done using the unpaired Student *t* test. The equality of variances was tested using the Levene's test. Two-tailed *P* values of 0.05 or less were considered to be statistically significant. The SPSS 10.0.1 program was utilized for the statistical analysis.

Western blot analysis

For RAGE western blotting analysis, protein was lysed into NP-40 protein lysis buffer (1% NP-40, 150 mM NaCl, 50 mM Tris–HCl, pH 7.4, and 100 μg of each aprotinin and leupeptin), and cell lysates were cleared of cell debris by centrifugation at 14,000 rpm (Eppendorf Bench Top Centrifuge) for 10 min at 4°C, separated on an 8% SDS-PAGE gel and electroblotted. The membrane was blocked with 5% milk for 1 h and then incubated for 2 h or overnight at 4°C with primary anti-RAGE antibody (Research Diagnostics Inc.), followed by HRP-conjugated secondary antibody. Immunoblots were developed with chemiluminescence reagents (Amersham).

For LRP-1 western blotting analysis, 600 μl of lysis buffer (1% Triton X-100, 10 mM Tris base, 5 mM EDTA, 50 mM NaCl, 30 mM tetra-sodium pyrophosphate, 50 mM sodium fluoride, 100 μl orthosodium vanadate, one complete ®protease inhibitor tablet per 10 ml, pH = 7.6) was added to 300 mg of human brain tissue. This was then mechanically homogenized using a Tekmar tissumizer. These samples were then centrifuged at 4°C at 14,000*g* for 10 min. Supernatant was then removed, and protein concentration was determined using the BioRad protein assay. Lysate of 75 μg was loaded in each lane of a 5% Tris–HCl gel and run under nonreducing conditions. The gel was then transferred to nitrocellulose. The nitrocellulose was then probed with a primary polyclonal antibody to LRP-1 (Orbigen Inc.) overnight at 4°C at a concentration of 2 μg/ml. Secondary HRP-labeled antibody was used to detect bound primary antibody and developed using

Amersham ECL detection reagents. The nitrocellulose was then exposed to Amersham hyperfilm ECL for 2 min and put into the developer.

Densitometry

Both RAGE and LRP-1 western blots were scanned with an Epson 636 scanner (Epson, Torrance, CA) and calibrated; densitometry measurements were preformed with NIH Image 1.62 (National Institutes of Health, Springfield VA).

All procedures involving experiments on human subjects are done in accord with the ethical standards of the Committee on the Protection of Human Subjects at Rhode Island Hospital (Federal Wide Assurance FWA00001230, assurance date 2005).

Results

Localization of RAGE and LRP-1 in normal aged control and AD hippocampus

We first examined the distribution of RAGE and LRP-1 within the hippocampi of both normal aged controls and AD brains. In control brains, there was robust RAGE immunoreactivity in neurons, whereas staining within the microvasculature was barely detectable (Fig. 1a, c). LRP-1 staining, in contrast, was clearly evident within brain microvessels but only weakly evident in neurons (Fig. 2a, c). In severe AD cases, neuronal RAGE immunoreactivity was almost completely lost (Fig. 1b). An unexpected finding was the strongly positive RAGE immunoreactivity within the microvasculature (Fig. 1d). A reversed pattern was evident for LRP-1 in AD. There was strong staining for LRP-1 in neurons, with minimal staining within the microvasculature (Fig. 2b, d). Thus, there is a shift in immunoreactivity between the neurons and vasculature for both RAGE and LRP-1. Robust RAGE immunoreactivity shifts from the neurons in control cases to the vasculature in AD cases. The reverse is true for LRP-1: robust immunoreactivity shifts from the vasculature in control cases to the neurons in AD cases.

Staining for both RAGE and LRP-1 within blood vessels was confirmed with double-labeling of either RAGE (Fig. 3) or LRP-1 (Fig. 4) with the endothelial cell marker CD31, while staining within neurons was confirmed with double-labeling of either RAGE (Fig. 5) or LRP-1 (Fig. 6) with neurofilament (NF).

We then looked for evidence of colocalization of RAGE and LRP-1 with Aβ in the AD cases. No evidence for colocalization of RAGE and Aβ was seen within either senile plaques or cerebral microvessels (Fig. 7). Unlike RAGE, colocalization of LRP-1 and Aβ was clearly present within senile plaques but not blood vessels (Fig. 8).

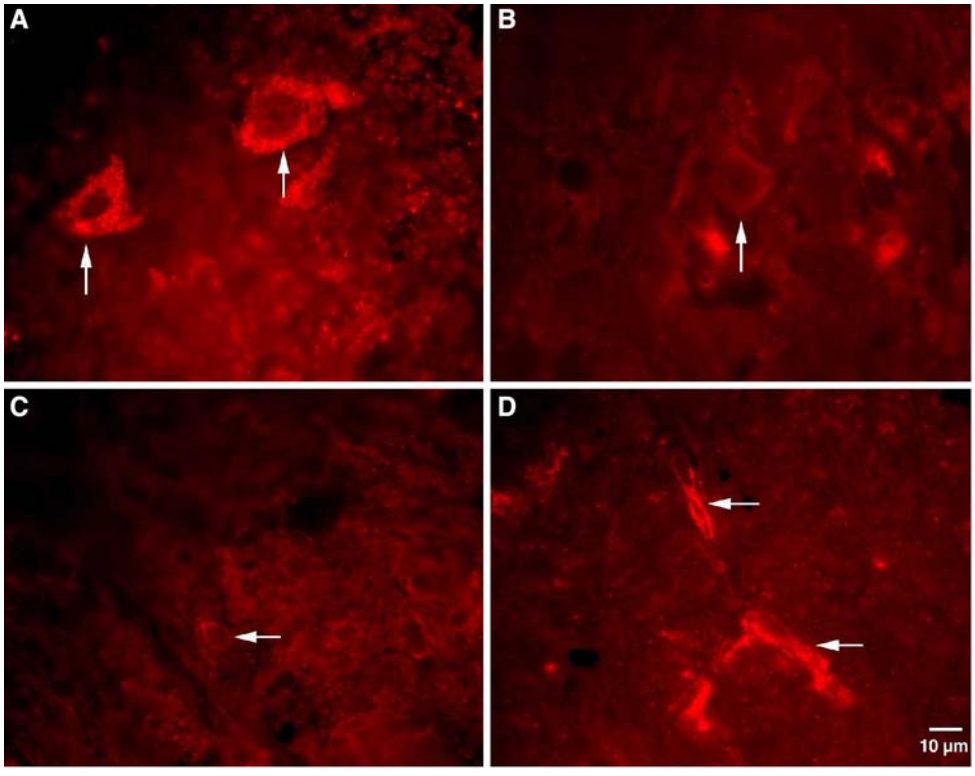

Fig. 1 Human hippocampal sections stained with RAGE antibody conjugated to Cy2. **a** and **c** represent control brains, while (**b**) and (**d**) represent AD brains. Note the robust neuronal staining (*arrows*) in control brains (**a**), compared with the relatively weak neuronal staining (*arrow*) in AD brains (**b**). Note also the weak microvascular staining (*arrow*) in control brains (**c**), compared with the robust vascular staining (*arrows*) in AD brains (**d**). Scale bar 10 μm

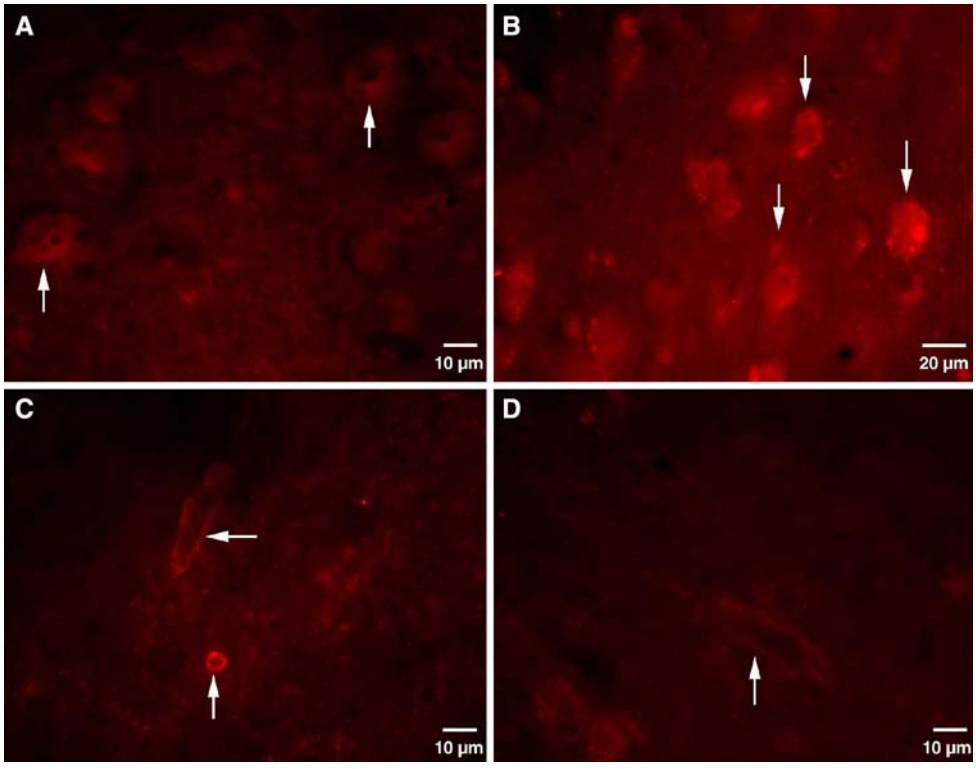

Fig. 2 Human hippocampal sections stained with LRP-1 antibody conjugated to Cy2. **a** and **c** represent control brains, while **(b)** and **(d)** represent AD brains. Note the weak neuronal staining (*arrows*) in control brains (**a**), compared with the robust neuronal staining (*arrows*) in AD brains (**b**). Note also the robust microvascular staining (*arrows*) in control brains (**c**), compared with the weak vascular staining (*arrow*) in AD brains (**d**). Scale bars are as indicated

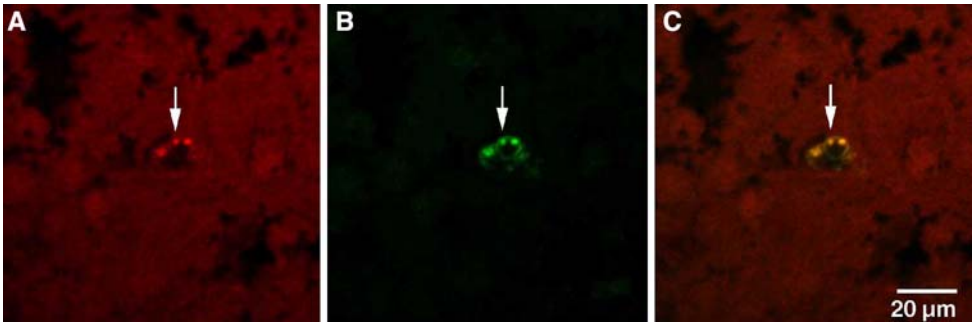

Fig. 3 Microvessel in section of human AD hippocampus stained with both RAGE (**a**) and CD31, an endothelial cell marker (**b**), antibodies conjugated to Cy3 and Cy2, respectively, and imaged using confocal microscopy. Both antibodies robustly stain the endothelial cells (*arrows*) and colocalize, as confirmed in the merged image (**c**). Scale bar 10 μm

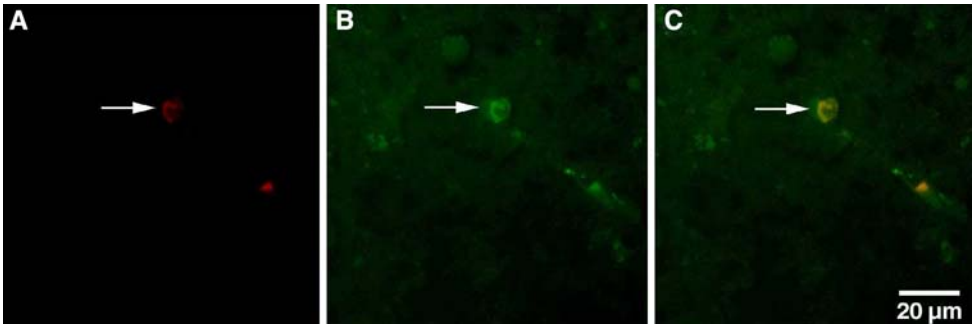

Fig. 4 Microvessel in section of human control hippocampus stained with both LRP-1 (**a**) and CD31, an endothelial cell marker (**b**), antibodies conjugated to Cy3 and Cy2, respectively, and imaged using confocal microscopy. Both antibodies robustly stain the endothelial cells (*arrows*) and colocalize, as confirmed in the merged image (**c**). Scale bar 20 μm

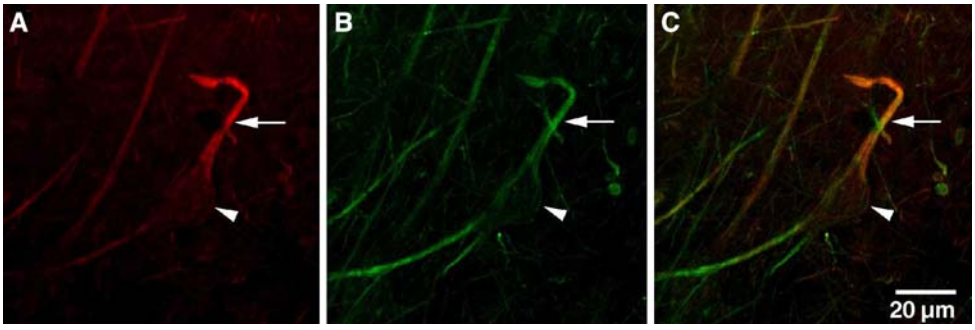

Fig. 5 Neuron in section of human control hippocampus stained with both RAGE (**a**) and neurofilament (**b**) antibodies conjugated to Cy3 and Cy2, respectively, and imaged using confocal microscopy. Both antibodies robustly stain neuronal processes (*arrows*) and colocalize, as confirmed in the merged image (**c**). The nucleus of the neuron is unstained (*arrowheads*). Scale bar 20 μm

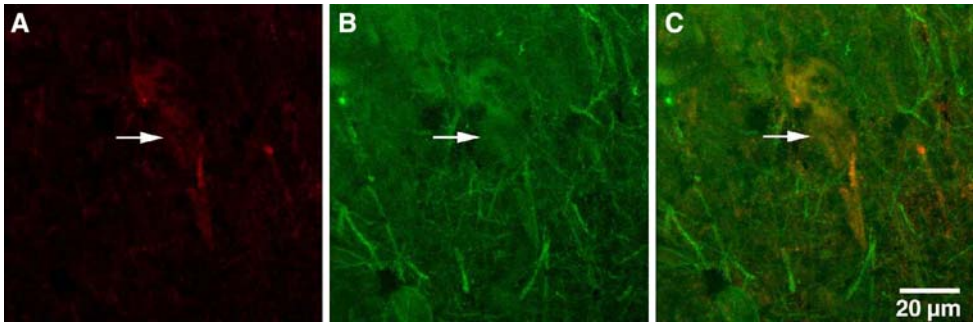

Fig. 6 Neuron in section of human AD hippocampus stained with both LRP-1 (**a**) and neurofilament (**b**) antibodies conjugated to Cy3 and Cy2, respectively, and imaged using confocal microscopy. Both antibodies robustly stain neuronal processes (*arrows*) and colocalize, as confirmed in the merged image (**c**). Scale bar 20 μm

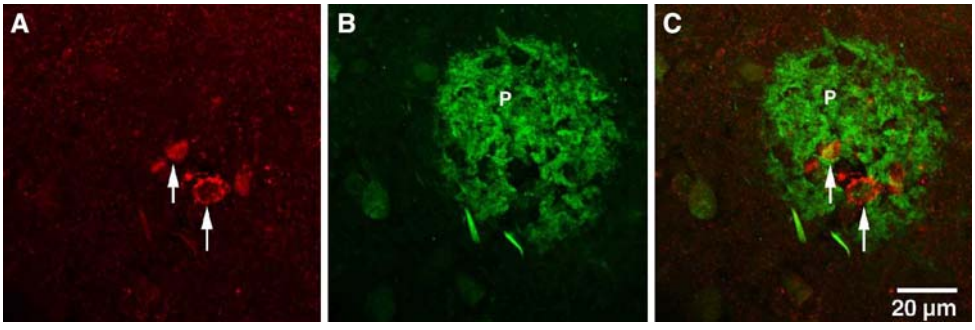

Fig. 7 Section of human AD hippocampus stained with both RAGE antibody conjugated to Cy3 (**a**) and thioflavin S for Aβ (**b**) and imaged using confocal microscopy. RAGE robustly stains the microvasculature (*arrows*), while Aβ is diffusely present within neuritic plaques (*P*). The merged image (**c**), however, reveals a lack of colocalization of RAGE and Aβ in either blood vessels or plaques. Scale bar 20 μm

Optical density quantification of RAGE and LRP-1 in normal aged control and AD hippocampus

Representative immunohistochemical photomicrographs that served as the basis of the quantitative studies are shown in Fig. 9. Optical density (OD) is measured in "gray level" units on a scale of 0–255, with an OD of "0" representing black (most densely-stained pattern) and "255" representing white (most lightly-stained pattern). Therefore, a lower OD indicates darker staining and thus increased positivity for a given antibody.

The results are depicted numerically in Tables 1 and 2 and graphically in Fig. 10. They confirm the observations noted above; namely, that RAGE immunoreactivity shifts from the neurons to the blood vessels and LRP-1 immunoreactivity from the blood vessels to the neurons in AD.

Western blot analysis

RAGE A representative western blot for RAGE is shown in Fig. 11a. A very large, strong band was present at 50 kDa in the control lung tissue and in the brain

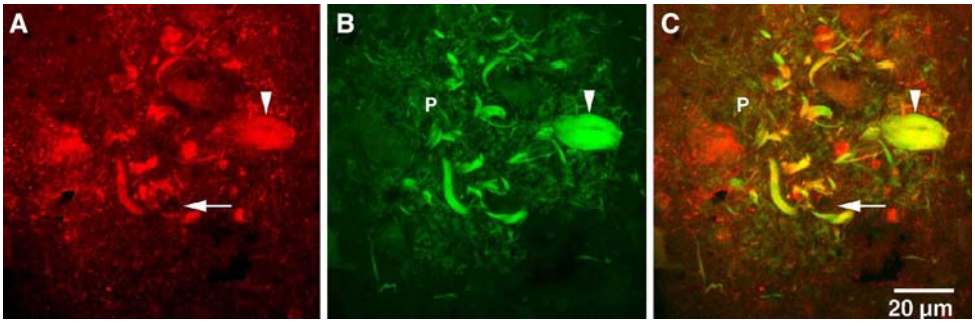

Fig. 8 Section of human AD hippocampus stained with both LRP-1 antibody conjugated to Cy3 (**a**) and thioflavin S for Aβ (**b**) and imaged using confocal microscopy. LRP-1 weakly stains the microvasculature (*arrows*), while Aβ is diffusely present within neuritic plaques (*P*). The merged image (**c**) reveals colocalization of LRP-1 and Aβ in the plaques (*yellow* staining), but not the vessels. The arrowhead represents a dystrophic neurite. Scale bar 20 μm

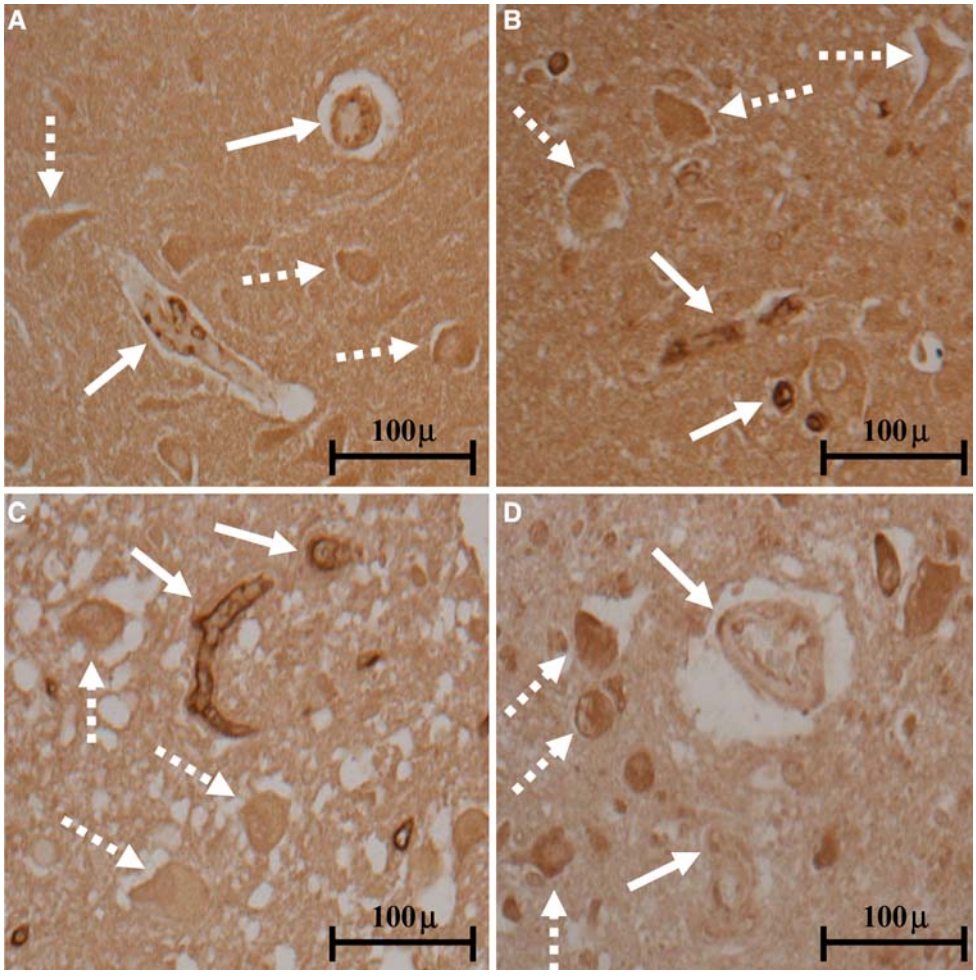

Fig. 9 RAGE and LRP-1 DAB immunohistochemical studies used in quantitative analysis. RAGE immunostaining in control hippocampus (**a**) shows mostly weak and fragmented reactivity in the vasculature (*solid arrows*) compared with neurons (*dotted arrows*), while in AD hippocampus (**b**), microvascular immunoreactivity (*solid arrows*) is much more intense then in neurons (*dotted arrows*). The reverse is true for LRP-1. LRP-1 immunostaining of control hippocampus (**c**) reveals much stronger reactivity in the microvasculature (*solid arrows*) than in neurons (*dotted arrows*), while in AD hippocampus (**d**), neuronal reactivity (*dotted arrows*) is much more intense than in the microvasculature (*solid arrows*). Scale bar 100 μm

homogenates, which corresponds to RAGE [28]. In human hippocampi, there was a much stronger band at 50 kDa in the AD hippocampus than in the control hippocampus, consistent with increased levels of RAGE in the vasculature of AD hippocampus as seen with immunofluorescence. In prefrontal cortex, the bands were not as strong as the hippocampus. The band for control cortex was stronger than for AD cortex, likely reflective of the enhanced neuronal levels in control neurons as noted with immunofluorescence. (As we showed above, neuronal levels of RAGE decrease in AD.) Quantitative densitometry analysis confirms the findings shown visually in the western blot; this is shown in Fig. 11b.

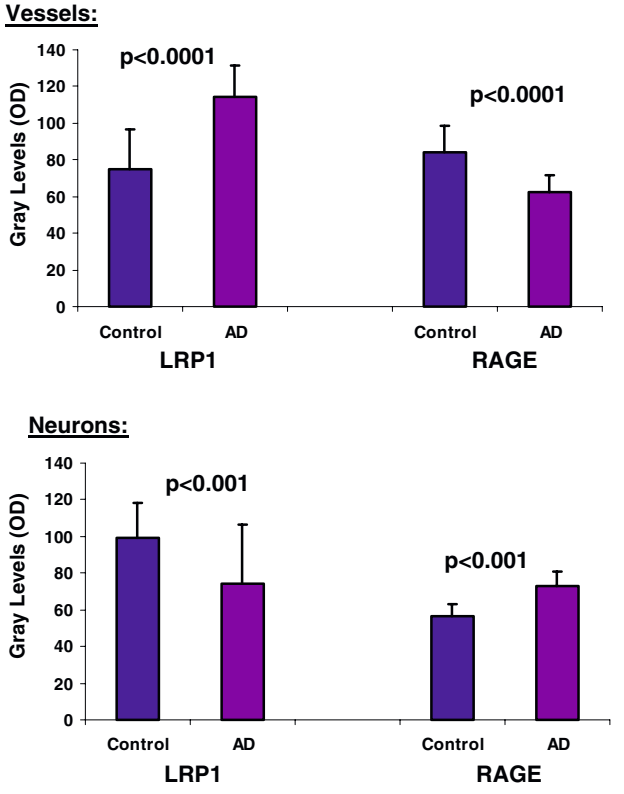

Fig. 10 *Top* Graphical representation of microvascular optical densities for both LRP-1 and RAGE. LRP-1 reactivity is significantly stronger (lower OD value) in control vessels than in AD vessels. The reverse is true for RAGE. *Bottom* Graphical representation of neuronal optical densities for both LRP-1 and RAGE. LRP-1 reactivity is significantly stronger (lower OD value) in AD neurons compared to control neurons. The reverse is true for RAGE

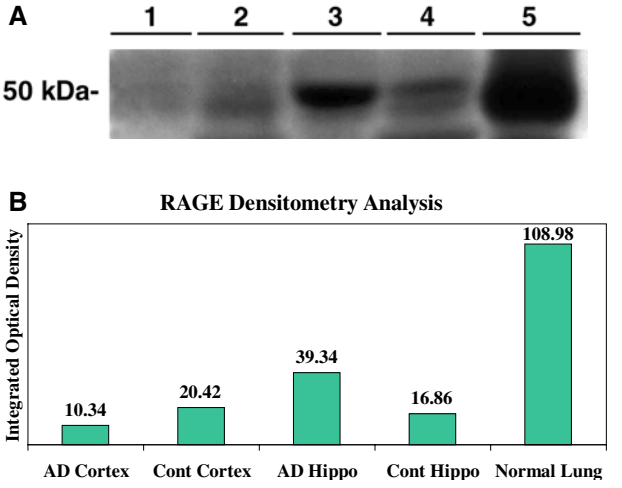

Fig. 11 **a** RAGE western blot. *Lane 1* prefrontal AD cortex. *Lane 2* prefrontal control cortex. *Lane 3* AD hippocampus. *Lane 4* control hippocampus. *Lane 5* normal lung. A much stronger signal is seen in AD hippocampus than in control hippocampus, while a somewhat stronger signal is noted in control cortex than in AD cortex. See text for details. **b** RAGE densitometry. This quantitative analysis of integrated optical density confirms the findings seen visually in the western blot; namely, there is increased RAGE seen in AD hippocampus than in control hippocampus, while more RAGE is present in control cortex than in AD cortex

Table 1 Quantitative immunohistochemical optical densities in the microvasculature for both RAGE and LRP-1 in AD and control hippocampi

	AD	Control	*P* value
RAGE	62.5 ± 9.2	84.2 ± 14.6	< 0.0001
LRP-1	114.6 ± 16.6	74.94 ± 21.7	< 0.0001

Table 2 Quantitative immunohistochemical optical densities in neurons for both RAGE and LRP-1 in AD and control hippocampi

	AD	Control	*P* value
RAGE	73.1 ± 8.0	56.8 ± 6.0	< 0.001
LRP-1	74.2 ± 32.0	99.0 ± 19.0	< 0.001

LRP-1 A representative western blot for LRP-1 is shown in Fig. 12a. A moderately strong band was present at 600 kDa in control lung and liver tissue, which corresponds to LRP-1 [7]. An unexpected finding was stronger bands in both AD hippocampus and prefrontal cortex, as compared with controls. These increased levels in AD cortex and hippocampus may partially be explained by the increased neuronal immunoreactivity of LRP-1 in AD. However, the main reason for the increased levels is the intimate association of LRP-1 with senile plaques in severe AD, as demonstrated by LRP-1 colocalization with Aβ in senile plaques (see above immunofluorescence results). Quantitative densitometry analysis confirms the findings shown visually in the western blot; this is shown in Fig. 12b.

Discussion

It has been suggested that one cause for amyloid accumulation in the brain of aged and AD patients is an age-related inability to clear Aβ from the brain [16, 19]. Two primary clearance routes from the brain exist for Aβ. The main route, in healthy young adults, is across the capillary endothelium; whereas a lesser amount is cleared via diffusion and bulk flow of interstitial fluid and CSF [22].

Aged primates show an accumulation of Aβ in blood vessel walls and in the perivascular brain tissue that appears to result from a loss of LRP-1 transport [10, 31]. It has also been shown that Aβ transport clearance across the BBB in mice decreases significantly

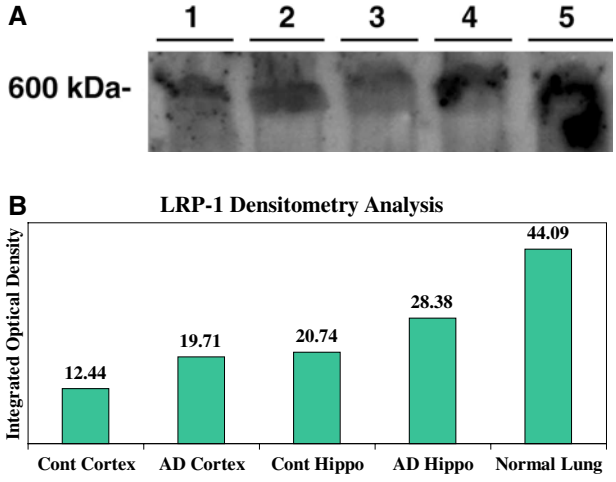

Fig. 12 **a** LRP-1 western blot. *Lane 1* prefrontal control cortex. *Lane 2* prefrontal AD cortex. *Lane 3* control hippocampus. *Lane 4* AD hippocampus. *Lane 5* normal lung. Stronger signals are seen in both AD cortex and hippocampus when compared with corresponding controls. See text for details. **b** LRP-1 densitometry. This quantitative analysis of integrated optical density confirms the findings seen visually in the western blot; namely, more LRP-1 is present in both AD cortex and hippocampus when compared with corresponding controls

with age. Comparing 3–9-month-old mice, there is a 50% decrease in LRP-1 function in the latter [20]. We have now shown not only that LRP-1 immunoreactivity on endothelial cells is reduced in AD, but there also appears to be an increase in endothelial RAGE immunoreactivity. Taken together, the result is a net increase in Aβ transport into the interstitial space of the brain in AD. This added Aβ is likely to be in excess of what can be removed via CSF turnover and clearance, which is also reduced in AD [21].

Work done in mice [6, 20] has provided strong support for the hypothesis that RAGE and LRP-1 perform opposite functions in transporting Aβ. RAGE transports Aβ into the brain, and LRP-1 transports Aβ out of the brain. Our experiments here indicate that severe AD is associated with significant changes in the relative distribution of RAGE and LRP-1 receptors in human hippocampus. Both the neuronal and vascular immunoreactivity of RAGE and LRP-1 are exactly reversed in severe AD, when compared to age-matched controls. The immunoreactivity of RAGE increases in microvascular endothelium and decreases on neurons, whereas that of LRP-1 decreases on endothelium and increases on neurons. Given the increase in RAGE and decrease in LRP-1 immunoreactivity in the AD cerebral microvasculature, one would expect to see a net flux of Aβ across the BBB from the plasma pool into the brain in AD, further worsening the brain amyloid burden.

We hypothesized an increase in total RAGE protein in whole brain homogenates of AD hippocampus in western blot analysis when compared to elderly controls, as seen in Fig. 11a. The immunofluorescence, quantitative immunohistochemical, and western blot data suggest not only a shift in the localization of RAGE receptors from neurons to capillary endothelial apical membranes, but also an increase in total RAGE protein (Fig. 11a, b). It is not yet clear whether this increase in capillary RAGE is due to an increase in expression locally, or results from an effect of increased soluble RAGE generated elsewhere. Because the immunoreactivity localizations of RAGE and LRP-1 are apparently reciprocal, as noted above, we expected LRP-1 levels to be decreased in whole brain homogenates of AD hippocampus when compared to controls. Thus, it was initially surprising to find that the levels of LRP-1 were actually increased in AD hippocampus (Fig. 12a, b). Although we showed by immunostaining that increased LRP-1 is present in AD neurons, that does not completely explain why total LRP-1 is increased in AD hippocampus, given that severe AD is associated with significant neuronal loss. The likely explanation is found in our LRP-1/Aβ colocalization experiment (Fig. 8), where we showed that LRP-1 colocalizes with Aβ in senile plaques. Total LRP-1 in whole brain homogenates of AD hippocampus increases because LRP-1 is intimately associated with the large numbers of senile plaques in our severe AD cases. Colocalization of LRP-1, but not RAGE, with Aβ in senile plaques suggests a possible relationship between the loss of capillary LRP-1, the increase in neuronal LRP-1, and the toxicity of Aβ. It has been suggested that LRP-1 on the endothelial cells of the blood–brain barrier, as well as on neurons, can mediate clearance of the toxic Aβ species, but this ultimately leads to their demise [8]. Reduction of Aβ efflux results from LRP-1/Aβ-mediated endothelial cell death; increased neuronal clearance of Aβ via LRP-1 with subsequent neuronal death may be one of the early events in the pathogenesis of AD [8, 30]. To further elucidate these changes that we have seen in AD hippocampus, we are in the process of preparing microvessel isolations of hippocampal cortex for RT-PCR and western blot analysis of both LRP-1 and RAGE.

Our results are similar to those obtained in other studies of human AD relating to either RAGE [17, 27] or LRP-1 [15, 20, 25, 26]. In one study [27], increased RAGE staining was seen immunohistochemically in the microvasculature of AD hippocampi, and increased quantity of RAGE was noted by ELISA in AD brain versus control. Another human RAGE study [17] focused on neuronal and astrocytic RAGE

immunoreactivity. Robust RAGE staining appears to be present in hippocampal neurons and astrocytes of brains with AD. The staining was also robust in control brains, and it was visually difficult to detect a difference between AD and control cases. That study used five AD and three control brains; however, the stage of the AD cases was not documented.

In the human tissue component of an LRP-1 study [20], reduced LRP-1 staining of the microvasculature was also noted in AD brains, similar to the findings in this investigation that characterizes the reciprocal relationship between RAGE and LRP-1. Other studies [15, 25, 26] have noted the presence of LRP-1 in normal neurons. While our study also notes the presence of LRP-1 in normal neurons, increased LRP-1 within AD neurons was seen in our study. As noted above, this may be a reactive phenomenon on the part of the neuron to attempt to clear Aβ from the brain. One of these studies [15] also demonstrated colocalization of LRP-1 in senile plaques, similar to what we observed in our study.

In conclusion, our data demonstrate that AD is associated with significant changes in the relative distribution of RAGE and LRP-1 receptors at the BBB in human hippocampus. The data also support the hypothesis that vascular amyloid deposition increases within the brains of AD patients. This implies that amyloid from the systemic circulation may be a major contributor to the brain amyloid burden in severe Alzheimer's disease.

Acknowledgments The authors wish to thank Tien Nguyen, Frederick Goulette, Anthony Spangenberger, and Mirna Lechpammer for their contributions in the preparation of this manuscript, as well as the Harvard Brain Tissue Resource Center (supported in part by PHS grant #R24MH068855) for supplying some of the tissues used in the experiments. The Rae and Jerry Richter Alzheimer's disease research fund also provided support for this manuscript

References

1. (1997) Consensus recommendations for the postmortem diagnosis of Alzheimer's disease The National Institute on Aging, and Reagan Institute Working Group on diagnostic criteria for the neuropathological assessment of Alzheimer's disease. Neurobiol Aging 18:S1–2
2. Braak H, Braak E (1991) Neuropathological staging of Alzheimer-related changes. Acta Neuropathol (Berl) 82:239–259
3. Cras P, Kawai M, Siedlak S, Mulvihill P, Gambetti P, Lowery D, Gonzalez-DeWhitt P, Greenberg B, Perry G (1990) Neuronal and microglial involvement in beta-amyloid protein deposition in Alzheimer's disease. Am J Pathol 137:241–246
4. Cummings BJ, Su JH, Geddes JW, Van Nostrand WE, Wagner SL, Cunningham DD, Cotman CW (1992) Aggregation of the amyloid precursor protein within degenerating neurons and dystrophic neurites in Alzheimer's disease. Neuroscience 48:763–777
5. D'Andrea MR, Nagele RG, Wang HY, Peterson PA, Lee DH (2001) Evidence that neurones accumulating amyloid can undergo lysis to form amyloid plaques in Alzheimer's disease. Histopathology 38:120–134
6. Deane R, Du YS, Submamaryan R, LaRue B, Jovanovic S, Hogg E, Welch D, Manness L, Lin C, Yu J, Zhu H, Ghiso J, Frangione B, Stern A, Schmidt A, Armstrong D, Arnold B, Liliensiek B, Nawroth P, Hofman F, Kindy M, Stern D, Zlokovic B (2003) RAGE mediates amyloid-beta peptide transport across the blood–brain barrier and accumulation in brain. Nat Med 9:907–913
7. Grimsley PG, Quinn KA, Chesterman CN, Owensby DA (1999) Evolutionary conservation of circulating soluble low density lipoprotein receptor-related protein-like ("LRP-like") molecules. Thromb Res 94:153–164
8. Harris-White ME, Frautschy SA (2005) Low density lipoprotein receptor-related proteins (LRPs), Alzheimer's and cognition. Curr Drug Targets CNS Neurol Disord 4:469–480
9. Herz J, Marschang P (2003) Coaxing the LDL receptor family into the fold. Cell 112:289–292
10. Mackic J, Stins M, McComb J, Calero M, Ghiso J, Kim K, Yan S, Stern D, Schmidt A, Frangione B, Zlokovic B (1998) Human blood–brain barrier receptors for Alzheimer's amyloid-beta 1–40 asymmetrical binding, endocytosis, and transcytosis at the apical side of brain microvascular endothelial cell monolayer. J Clin Invest 102:734–743
11. Monro OR, Mackic JB, Yamada S, Segal MB, Ghiso J, Maurer C, Calero M, Frangione B, Zlokovic BV (2002) Substitution at codon 22 reduces clearance of Alzheimer's amyloid-beta peptide from the cerebrospinal fluid and prevents its transport from the central nervous system into blood. Neurobiol Aging 23:405–412
12. Pluta R, Barcikowska M, Januszewski S, Misicka A, Lipkowski A (1996) Evidence of blood–brain barrier permeability/leakage for circulating human Alzheimer's beta-amyloid-(1–42)-peptide. Neuroreport 7:1261–1265
13. Poduslo J, Curran G, Sanyal B, Selkoe D (1999) Receptor-mediated transport of human amyloid beta-protein 1–40 and 1–42 at the blood–brain barrier. Neurobiol Dis 6:190–199
14. Powers J, Skeen J (1988) Ultrastructural heterogeneity in cerebral amyloid of Alzheimer's disease. Acta Neuropathol (Berl) 76:613–623
15. Rebeck GW, Reiter JS, Strickland DK, Hyman BT (1993) Apolipoprotein E in sporadic Alzheimer's disease: allelic variation and receptor interactions. Neuron 11:575–580
16. Rubenstein E (1998) Relationship of senescence of cerebrospinal fluid circulatory system to dementias of the aged. Lancet 351:283–285
17. Sasaki N, Toki S, Chowei H, Saito T, Nakano N, Hayashi Y, Takeuchi M, Makita Z (2001) Immunohistochemical distribution of the receptor for advanced glycation end products in neurons and astrocytes in Alzheimer's disease. Brain Res 888:256–262
18. Selkoe DJ (1989) Molecular pathology of amyloidogenic proteins and the role of vascular amyloidosis in Alzheimer's disease. Neurobiol Aging 10:387–395
19. Selkoe DJ (2000) Toward a comprehensive theory for Alzheimer's disease. Hypothesis: Alzheimer's disease is caused by the cerebral accumulation and cytotoxicity of amyloid beta-protein. Ann N Y Acad Sci 924:17–25
20. Shibata M, Yamada S, Kumar S, Calero M, Bading J, Frangione B, Holtzman D, Miller C, Strickland D, Ghiso J, Zlokovic B (2000) Clearance of Alzheimer's amyloid-ss(1–40) peptide from brain by LDL receptor-related protein-1 at the blood–brain barrier. J Clin Invest 106:1489–1499

21. Silverberg GD, Heit G, Huhn S, Jaffe RA, Chang SD, Bronte-Stewart H, Rubenstein E, Possin K, Saul TA (2001) The cerebrospinal fluid production rate is reduced in dementia of the Alzheimer's type. Neurology 57:1763–1766
22. Silverberg GD, Mayo M, Saul T, Rubenstein E, McGuire D (2003) Alzheimer's disease, normal-pressure hydrocephalus, and senescent changes in CSF circulatory physiology: a hypothesis. Lancet Neurol 2:506–511
23. Siman R, Card JP, Nelson RB, Davis LG (1989) Expression of beta-amyloid precursor protein in reactive astrocytes following neuronal damage. Neuron 3:275–285
24. Stewart PA, Hayakawa K, Akers MA, Vinters HV (1992) A morphometric study of the blood–brain barrier in Alzheimer's disease. Lab Invest 67:734–742
25. Tooyama I, Kawamata T, Akiyama H, Kimura H, Moestrup SK, Gliemann J, Matsuo A, McGeer PL (1995) Subcellular localization of the low density lipoprotein receptor-related protein (alpha 2-macroglobulin receptor) in human brain. Brain Res 691:235–238
26. Wolf BB, Lopes MB, VandenBerg SR, Gonias SL (1992) Characterization and immunohistochemical localization of alpha 2-macroglobulin receptor (low-density lipoprotein receptor-related protein) in human brain. Am J Pathol 141:37–42
27. Yan SD, Chen X, Fu J, Chen M, Zhu H, Roher A, Slattery T, Zhao L, Nagashima M, Morser J, Migheli A, Nawroth P, Stern D, Schmidt AM (1996) RAGE and amyloid-beta peptide neurotoxicity in Alzheimer's disease. Nature 382:685–691
28. Yan SD, Stern D, Kane MD, Kuo YM, Lampert HC, Roher AE (1998) RAGE-Abeta interactions in the pathophysiology of Alzheimer's disease. Restor Neurol Neurosci 12:167–173
29. Yan SD, Zhu H, Zhu A, Golabek A, Du H, Roher A, Yu J, Soto C, Schmidt AM, Stern D, Kindy M (2000) Receptor-dependent cell stress and amyloid accumulation in systemic amyloidosis. Nat Med 6:643–651
30. Zerbinatti CV, Bu G (2005) LRP and Alzheimer's disease. Rev Neurosci 16:123–135
31. Zlokovic B (1997) Can blood–brain barrier play a role in the development of cerebral amyloidosis and Alzheimer's disease pathology. Neurobiol Dis 4: 23–26
32. Zlokovic BV (2004) Clearing amyloid through the blood–brain barrier. J Neurochem 89:807–811